

Patterns of interval correlations in neural oscillators with adaptation

Tilo Schwalger^{1,2} and Benjamin Lindner^{1,2}

¹*Bernstein Center for Computational Neuroscience, Haus 2, Philippstr 13, 10115 Berlin, Germany*

²*Department of Physics, Humboldt Universität zu Berlin, Newtonstr 15, 12489 Berlin, Germany*

(Dated: March 6, 2013)

Neural firing is often subject to negative feedback by adaptation currents. These currents can induce strong correlations among the time intervals between spikes. Here we study analytically the interval correlations of a broad class of noisy neural oscillators with spike-triggered adaptation. Our weak-noise theory provides a general relation between the correlations and the phase-response curve of the oscillator, gives intuition about the sign of the correlations, and predicts a variety of correlation patterns that depend on the nonlinear dynamics of the model. At high firing rates, the long-term variability associated with the cumulative interval correlations becomes small, independent of model details. Our results are verified by comparison with stochastic simulations of the exponential, leaky, and generalized integrate-and-fire models with adaptation.

The nerve cells of the brain generate action potentials (spikes) by a nonlinear, adaptive, and noisy mechanism. In order to understand neural signal processing in single neurons it is vital to analyze the sequence of the inter-spike intervals (ISIs) between adjacent action potentials. There is experimental evidence accumulating that the spiking in many cases is *not* a renewal process, i.e. a spike train with mutually independent ISIs but that intervals are typically correlated over a few lags [1, 2]. Such correlations are often characterized by the serial correlation coefficient (SCC)

$$\rho_k = \frac{\langle (T_i - \langle T_i \rangle)(T_{i+k} - \langle T_{i+k} \rangle) \rangle}{\langle (T_i - \langle T_i \rangle)^2 \rangle}, \quad (1)$$

where T_i and T_{i+k} are two ISIs lagged by an integer k and $\langle \cdot \rangle$ denotes ensemble averaging.

An ubiquitous mechanism for ISI correlations are slow feedback processes mediating spike-frequency adaptation [3, 4]. These adaptation currents are typically associated with short-range correlations with a negative SCC at lag $k = 1$ and a reduced Fano factor as demonstrated by several numerical [5–8] and analytical studies [9–12]. However, a simple theory that predicts and explains possible correlation patterns is still lacking.

In this letter, we present a relation between the ISI correlation coefficient ρ_k and a basic characteristics of nonlinear neural dynamics, the *phase-response curve* (PRC). The PRC quantifies the advance (or delay) of the next spike caused by a small depolarizing current applied at the time t after the last spike. For neurons which integrate up their input (integrator neurons), the PRC is positive at all times (type I resetting) whereas neurons, which show subthreshold resonances (resonator neuron), possess a PRC that is partly negative (type II resetting) [13, 14]. Below we show that resonator neurons possess a richer repertoire of correlation patterns than integrator neurons do.

Model. Spike frequency adaptation can be modeled by Hodgkin-Huxley type neurons with a depolarization-activated adaptation current [6, 15, 16]. However, the

spiking of such conductance-based models can in many instances be approximated by simpler multi-dimensional integrate-fire (IF) models that are equipped with a spike-triggered adaptation current [17]; adapting IF models perform excellently in predicting spike times of real cells under noisy stimulation [18]. Here, we consider a stochastic nonlinear multi-dimensional IF model for the membrane potential v , N auxiliary variables w_j ($j = 1, \dots, N$) and a spike-triggered adaption current $a(t)$:

$$\dot{v} = f_0(v, \mathbf{w}) + \mu - a + \xi(t), \quad \dot{w}_j = f_j(v, \mathbf{w}), \quad (2a)$$

$$\tau_a \dot{a} = -a + \tau_a \Delta \sum_i \delta(t - t_i). \quad (2b)$$

The membrane potential $v(t)$ is subject to weak Gaussian noise $\xi(t)$ with $\langle \xi(t)\xi(t') \rangle = 2D\delta(t - t')$ and noise intensity D . The dynamics is complemented by a spike-and-reset mechanism: whenever $v(t)$ reaches a threshold v_T , a spike is registered at time $t_i = t$ and $v(t)$ and $\mathbf{w}(t) = [w_1(t), \dots, w_N(t)]^T$ are reset to $v(t_i+) = 0$ and $\mathbf{w}(t_i+) = \mathbf{w}_r$; $a(t)$ suffers a jump by Δ as seen from Eq. (2b), which resembles high-threshold adaptation currents [6, 7]. The constant input current μ is assumed to be sufficiently large to ensure ongoing spiking even in the absence of noise.

An important special case, the adaptive exponential integrate-and-fire model is illustrated in Fig.1 (here, $f_0(v) = -\gamma v + \gamma \Delta_T \exp[(v - 1)/\Delta_T]$ and $N = 0$). Time courses of $v(t)$ and $a(t)$ are shown in Fig.1a1,b1 for two distinct correlation patterns possible in this model. The ISI sequence T_i, T_{i+1}, T_{i+2} displays patterns of *short-long-long* (Fig.1a1) and *short-long-short* (Fig.1b1), corresponding to a negative SCC, which decays monotonically with the lag k (Fig.1a3) or to an SCC oscillating with k (Fig.1b3). Below we develop a theory to analyze these and other correlation patterns possible in multi-dimensional adapting IF models.

Theory. In our model Eq. (2), $a(t)$ is the only variable that keeps a memory of the previous spike times thereby

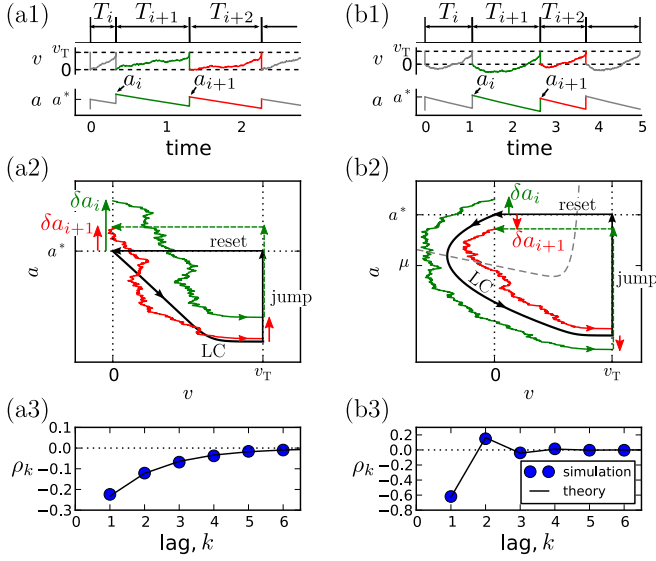


FIG. 1: Correlation patterns in the adaptive exponential IF model with $\tau_a = 10, \gamma = 1, \Delta_T = 0.1, v_T = 2, D = 0.1$. Adaptation is weak ($\Delta = 1, \mu = 15$) in (a) and strong ($\Delta = 10, \mu = 80$) in (b). Membrane voltage $v(t)$ and adaptation variable $a(t)$ with ISI sequences $\{T_i\}$ and peak adaptation values $\{a_i\}$ are shown in (a1,b1). Colored pieces of trajectories in the phase plane (v, a) in (a2,b2) correspond to the respective colors in (a1,b1); deterministic limit cycle (LC) is indicated by a thick black line. For weak adaptation (a2) a short ISI T_i causes positive deviations $\delta a_i = a_i - a^*$ and $\delta a_{i+1} = a_{i+1} - a^*$ of peak values leading to long ISIs T_{i+1} and T_{i+2} and, hence, to a negative ISI correlation at all lags (a3). Because of the qualitatively different limit cycle for strong adaptation (b2), deviations δa_i and δa_{i+1} differ in sign, yielding an oscillatory correlation pattern (b3).

inducing correlations between ISIs. Over one ISI the time course of adaptation is an exponential decay, relating two adjacent peak values a_i and a_{i+1} of $a(t)$ by

$$a_{i+1} = a_i e^{-T_{i+1}/\tau_a} + \Delta. \quad (3)$$

We assume that in the deterministic case ($D = 0$) our model has a finite period T^* (i.e. the model operates in the tonically firing regime) and, hence, for $D = 0$ the map (3) has a stable fixed point

$$a^* = \Delta / [1 - \exp(-T^*/\tau_a)]. \quad (4)$$

The asymptotic deterministic dynamics can be interpreted as a limit-cycle like motion in the phase space from the reset point to the threshold and back by the instantaneous reset (cf. Fig.1a2,b2).

Weak noise will cause small deviations in the period $\delta T_i = T_i - T^* \approx T_i - \langle T_i \rangle$ that are mutually correlated with coefficient ρ_k . The peak adaptation values, however, also fluctuate, $\delta a_i = a_i - a^*$, and both deviations are related by linearizing Eq. (3):

$$\delta T_{i+1} = \frac{\tau_a}{a^*} \left(\delta a_i - e^{T^*/\tau_a} \delta a_{i+1} \right). \quad (5)$$

A second relation between the small deviations can be gained by considering how a small perturbation affects the length of the period. This effect is captured by the infinitesimal phase response curve (PRC), $Z(t)$, $t \in (0, T^*)$ [13, 14]. In our case, the perturbation $\xi(t) - \delta a_i \exp(-(t - t_i)/\tau_a)$ comprises the weak noise and the deviation in the adaptation during (t_i, t_{i+1}) :

$$\delta T_{i+1} = \int_0^{T^*} dt Z(t) \left(\delta a_i e^{-\frac{t}{\tau_a}} - \xi(t_i + t) \right). \quad (6)$$

Combining Eqs. (5), (6) we obtain the stochastic map

$$\delta a_{i+1} = \alpha \vartheta \delta a_i + \Xi_i, \quad (7)$$

where $\Xi_i = -\frac{\alpha a^*}{\tau_a} \int_0^{T^*} dt Z(t) \xi(t_i + t)$ are uncorrelated random numbers and

$$\alpha = e^{-T^*/\tau_a}, \quad \vartheta = 1 - \frac{a^*}{\tau_a} \int_0^{T^*} dt Z(t) e^{-\frac{t}{\tau_a}}. \quad (8)$$

Note that local stability of the fixed point a^* requires that $|\alpha \vartheta| < 1$. The covariance $c_k = \langle \delta a_i \delta a_{i+k} \rangle$ of the auto-regressive process Eq. (7) can be calculated by elementary means and using Eq. (5) we obtain for $k \geq 1$:

$$\rho_k = -A(1 - \vartheta)(\alpha \vartheta)^{k-1}, \quad A = \frac{\alpha(1 - \alpha^2 \vartheta)}{1 + \alpha^2 - 2\alpha^2 \vartheta}. \quad (9)$$

In order to compute α and ϑ via Eq. (8), we have to calculate T^* and $Z(t)$ (a^* then follows from Eq. (4)), which can be done for simple systems analytically.

Our main result, Eqs. (8),(9), shows that the SCC is always a geometric sequence with respect to the lag k that can generate qualitatively different correlation patterns depending on the value of ϑ and thus on PRC and adaptation current. Because $|\alpha \vartheta| < 1$ and $0 < \alpha < 1$, the prefactor A in Eq. (9) is always positive. Consequently, ρ_1 is negative for $\vartheta < 1$ and positive for $\vartheta > 1$. The sign of higher lags is determined by the base of the power: for $\vartheta > 0$ correlations decay monotonically, whereas for $\vartheta < 0$ the SCC oscillates. Two special cases are $\vartheta = 0$ with a negative correlation at lag 1 and vanishing correlations at all higher lags and $\vartheta = 1$ where all correlations vanish. Our geometric formula covers all patterns of interval correlations that have been theoretically studied [9, 19], including the perfect IF model [11].

The cumulative effect of the correlations can be described by the sum over all ρ_k that is related to the long-time limit of the Fano factor and the low-frequency limit of the spike train power spectrum. It is given by

$$\sum_{k=1}^{\infty} \rho_k = -\frac{A(1 - \vartheta)}{1 - \alpha \vartheta} \simeq -\frac{1}{2} + \frac{1/2}{(1 + \Delta \tau_a / v_T)^2}, \quad (10)$$

where the latter expression is valid at high firing rates with $T^* \ll \tau_a$, achieved by a strong input current μ . In particular, for strong adaptation ($\Delta \tau_a \gg v_T$) the sum is

only slightly larger than $-1/2$ (for $-1/2$ the Fano factor, and hence the long-term variability vanishes).

One-dimensional IF models with adaptation. In the simplest case ($N = 0$, $f_0(v, \mathbf{w}) = f(v)$) the PRC reads

$$Z(t) = Z(T^*) \exp \left[\int_t^{T^*} dt' f'(v_0(t')) \right], \quad (11)$$

where $v_0(t)$ is the limit cycle solution and $Z(T^*) = [f(v_T) + \mu - a^* + \Delta]^{-1}$ is the inverse of the velocity $\dot{v}_0(T^*)$ at the threshold, which is always positive. Thus, the PRC is positive for all $t \in (0, T^*)$, i.e. 1D-IF models show type I behavior. Looking at Eq. (8) we find that a positive PRC inevitably yields $\vartheta < 1$ and hence implies $\rho_1 < 0$. Intuitively, a short ISI causes in the following on average a higher inhibitory adaptation during the subsequent ISI. Such an inhibitory current always enlarges the ISI in type I neurons – hence, a short ISI is followed by a long ISI.

The sign of the correlations at higher lags can be inferred from the sign of ϑ , for which one can show that $\vartheta = (f(0) + \mu - a^*)Z(0)$. Because $Z(0) > 0$, the sign of ϑ is determined by the sign of $f(0) + \mu - a^*$. For sufficiently small Δ (weak adaptation, see Fig. 1a) we will have $a^* < f(0) + \mu$, consequently, $\vartheta > 0$ and a negative correlation at all lags (Fig. 1a3). In this case, a short ISI occurring by fluctuation will cause a positive deviation δa_i (Fig. 1a2, green arrow). Geometrically, it is plausible that such a positive deviation causes a likewise positive deviation δa_{i+1} in the subsequent cycle (Fig. 1a2, red arrow). Because a positive deviation is associated with a long ISI, the initial short ISI is on average followed by longer ISIs.

In marked contrast, if Δ is sufficiently large (strong adaptation) such that $a^* > f(0) + \mu$, ϑ becomes negative and hence the SCC's sign alternates with the lag. This alternation of the sign can be understood by means of the phase plane. Let us again consider a positive deviation δa_i due to a short preceding ISI (Fig. 1b2, green arrow). Because $\dot{v}_0(0) = f(0) + \mu - a^* < 0$, the neuron hyperpolarizes at the beginning of the interval (i.e. the trajectory moves left into the region of negative voltage). At the turning point of the limit cycle the deviation of the adaptation reverses its sign, and hence δa_{i+1} becomes negative (Fig. 1(b2), red arrow). Because a positive (negative) deviation corresponds on average to a long (short) ISI, the alternation of δa_i also entails an alternation of the ISI correlations.

As demonstrated in Fig. 1a3, b3, our theory works well for the adapting exponential integrate-and-fire model. We next demonstrate the validity of our approach over a broad range of firing rates (Fig. 2) for another important 1D model, the adapting leaky integrate-and-fire model [20] for which $f(v) = -\gamma v$ and

$$Z(t) = \exp[\gamma(t - T^*)]/(\mu - \gamma v_T - a^* + \Delta) \quad (12)$$

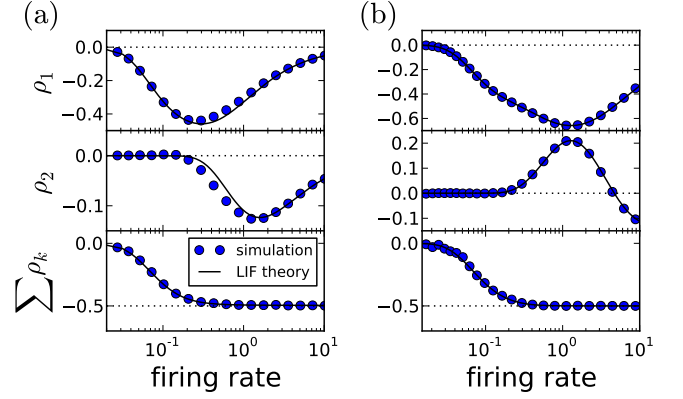


FIG. 2: ISI correlations of the adapting LIF model vs. firing rate $1/\langle T_i \rangle \approx 1/T^*$ where the rate is varied by increasing μ . The panels display (from top to bottom) ρ_1 , ρ_2 and the sum $\sum_{k=1}^m \rho_k$ for simulation (circles, $m = 100$) and theory (solid lines, $m \rightarrow \infty$). (a) Moderate adaptation: $\Delta = 1$, (b) strong adaptation: $\Delta = 10$. Both: $\gamma = 1$, $\tau_a = 10$, $D = 0.1$, $v_T = 1$.

(here T^* has still to be determined from a transcendental equation). Changing the firing rate by varying the input current μ , we find a good agreement for the first two correlation coefficients and the sum of all ρ_k . In accordance with previous findings [6–9, 11, 19, 21], the first correlation coefficient ρ_1 displays a minimum corresponding to strong anti-correlations between adjacent intervals. The correlations at lag 2 can be positive for a finite range of firing rates if the adaptation strength Δ is sufficiently large (Fig. 2(b)), whereas for moderate Δ we find a negative ρ_2 at all firing rates (Fig. 2(a)). In both cases, however, the sum of SCCs approaches a value close to $-1/2$ for high firing rates as predicted by Eq. (10) (Fig. 2, bottom). This is strikingly similar to experimental data from weakly electric fish, in which some electro-receptors display a monotonically decaying SCC and some show an oscillatory SCC [4] but all cells exhibit a sum close to $-1/2$ [22].

Adapting GIF model. Different correlation patterns become possible if we consider a type II PRC, which is by definition partly negative and can lead to a negative value of the integral in Eq. (8), and hence to $\vartheta \geq 1$. This corresponds to a non-negative SCC at lag 1, which is infeasible in the one-dimensional case. To test the prediction $\rho_1 \geq 0$, we study the generalized integrate-and-fire (GIF) model [23] (also known as resonate-and-fire model [24]), which is defined by $f_0(v, w) = -\gamma v - \beta w$ and $f_1(v, w) = v - w$. For this model, we find

$$Z(t) = \frac{e^{\frac{\nu}{2}(t-T^*)} \left[\cos(\Omega(t-T^*)) - \frac{1-\tau_w\gamma}{2\tau_w\Omega} \sin(\Omega(t-T^*)) \right]}{\mu - \gamma v_T - \beta w_0(T^*) - a^* + \Delta} \quad (13)$$

where $\nu = \gamma + 1/\tau_w$, $\Omega = \sqrt{\frac{\beta+\gamma}{\tau_w} - \frac{\nu^2}{4}}$ and $w_0(t)$ is one component of the deterministic limit-cycle solution

$[v_0(t), w_0(t), a_0(t)]$ that we calculated numerically.

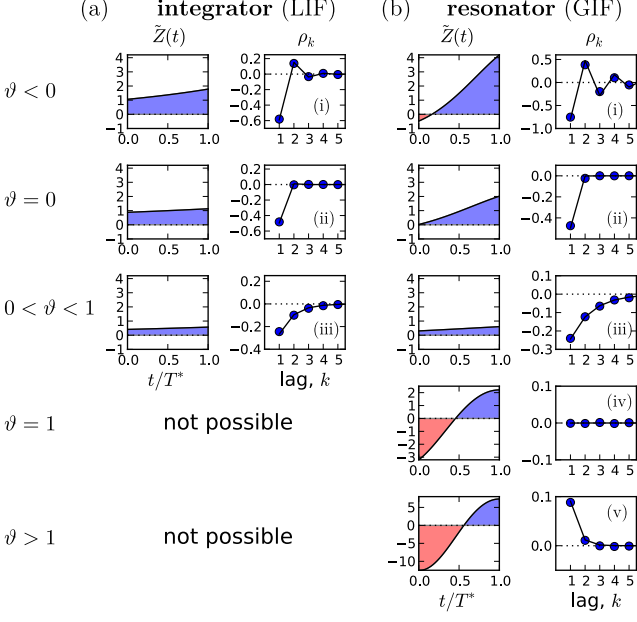


FIG. 3: Possible correlation patterns and corresponding PRCs. For the adapting LIF model (a), $\vartheta < 1$ and only three qualitative different cases are possible. The adapting GIF model (b) exhibits the full repertoire of correlation patterns because the PRC can be partly negative and ϑ can attain values from its entire physically meaningful interval $[-1/\alpha, 1/\alpha]$. The value of ϑ and hence the type of correlation pattern is set by the integral over the weighted PRC $\tilde{Z}(t) = Z(t)e^{-\frac{t}{\tau_a} \frac{a^* T^*}{\tau_a}}$, shown in left panels. LIF parameters: $D = 0.1$, $\tau_a = 2$, (i) $\mu = 20$, $\Delta = 10$, (ii) $\mu = 20$, $\Delta = 4.47$, (iii) $\mu = 5$, $\Delta = 1$. GIF parameters: (i) $\mu = 10$, $\beta = 3$, $\tau_a = 10$. (ii) $\mu = 11.75$, $\beta = 3$, $\tau_a = 10$. (iii) $\mu = 20$, $\beta = 1.5$, $\tau_a = 10$. (iv) $\mu = 2.12$, $\beta = 1.5$, $\tau_a = 1$, $\Delta = 10$. (v) $\mu = 1.5$, $\beta = 1.5$, $\tau_a = 1$, $\Delta = 9$, $D = 10^{-5}$. Unless stated otherwise, $\gamma = 1$, $\Delta = 1$, $\tau_w = 1.5$, $D = 10^{-4}$, $w_r = 0$.

In Fig. 3b we demonstrate that all possible correlation patterns can be realized in the GIF model and that the predicted SCCs agree quantitatively well in theory and model simulations (for comparison, see the SCC for the LIF in Fig. 3a). To each distinct pattern belongs a range of ϑ (Fig. 3, left), determined by the area under the weighted PRC $\tilde{Z}(t) = \frac{a^*}{\tau_a} e^{-\frac{t}{\tau_a} \frac{a^* T^*}{\tau_a}} Z(t)$. The function $\tilde{Z}(t)$ (left column in Fig. 3a,b) illustrates, why an adapting GIF neuron can show vanishing (Fig. 3b(iv)) or even *purely positive* ISI correlations (Fig. 3b(v)). In case of type II resetting, inhibitory input can *shorten* the ISI because of the negative part in the PRC; here inhibition acts like an excitatory input. Consequently, a short ISI will induce a stronger inhibition (adaptation) that now causes a likewise short interval and results thus in a positive correlation between adjacent ISIs. Also, the shortening effect of the adaption current in the early negative phase of the PRC can be exactly balanced by the delaying effect of the late positive phase of the PRC

(pseudo-renewal case, in which the area under \tilde{Z} is zero).

Conclusions. We have found a general relation between two experimentally accessible characteristics: the serial interval correlations and the phase response curve of a noisy neuron with spike-triggered adaptation. Our analytical results require that the noise is weak but are valid for arbitrary adaptation strength and time scale. The theory predicts distinct correlation patterns like short-range negative and oscillatory correlations that have been observed in experiments [4, 25] and in simulation studies of adapting neurons [3, 7]. Beyond negative and oscillatory correlations, we have found, however, that resonator neurons with spike-frequency adaptation can exhibit purely positive ISI correlations or a pseudo-renewal process with uncorrelated intervals. Adaptation currents that are commonly associated with negative ISI correlations can thus induce a richer repertoire of correlation patterns than previously thought. Despite the multitude of patterns, there is a universal limit for the cumulative correlations at high firing rates (cf. Eq. (10)), which shows that the long-term variability is in this limit always reduced in agreement with experimental studies [22].

As an outlook we sketch, how our theory could be used to constrain unknown physiological parameters by measured correlation coefficients and phase response curves. For instance, from the mean ISI we can estimate $T^* = \langle T \rangle$. Furthermore, knowing $\rho_1 = -A(\alpha, \vartheta)(1 - \vartheta)$ as well as the ratio $\rho_2/\rho_1 = \alpha\vartheta$ one can eliminate ϑ and solve for α . This allows to estimate the unknown adaptation time constant $\tau_a = -T^*/\ln \alpha$ and the amplitude of the adaptation current

$$a^* = \frac{\tau_a}{\alpha} \left(\alpha - \frac{\rho_2}{\rho_1} \right) \bigg/ \int_0^{T^*} dt Z(t) e^{-\frac{t}{\tau_a}}. \quad (14)$$

Although experimental PRCs are notoriously noisy [13], the integral over $Z(t)$ determining our estimate of a^* is less error-prone. Combining our approach with advanced estimation methods for the PRC [26], may thus provide an alternative access to hidden physiological parameters using only spike time statistics.

-
- [1] F. Farkhooi, M. F. Strube-Bloss, and M. P. Nawrot, Phys. Rev. E **79**, 021905 (2009).
 - [2] O. Avila-Akerberg and M. J. Chacron, Experimental Brain Research (2011).
 - [3] M. J. Chacron, A. Longtin, M. St-Hilaire, and L. Maler, Phys. Rev. Lett. **85**, 1576 (2000).
 - [4] R. Ratnam and M. E. Nelson, J. Neurosci. **20**, 6672 (2000).
 - [5] C. Geisler and J. M. Goldberg, Biophys. J. **6**, 53 (1966).
 - [6] X. J. Wang, J Neurophysiol **79**, 1549 (1998).
 - [7] Y.-H. Liu and X.-J. Wang, J. Comp. Neurosci. **10**, 25 (2001).

- [8] J. Benda, L. Maler, and A. Longtin, *J Neurophysiol* **104**, 2806 (2010).
- [9] E. Urdapilleta, *Phys Rev E* **84**, 041904 (2011).
- [10] F. Farkhooi, E. Muller, and M. P. Nawrot, *Phys. Rev. E* **83**, 050905 (2011).
- [11] T. Schwalger, K. Fisch, J. Benda, and B. Lindner, *PLoS Comput Biol* **6**, e1001026 (2010).
- [12] C. van Vreeswijk, in *Analysis of Parallel Spike Trains*, edited by S. Grün and S. Rotter (Springer, 2010), chap. 1.
- [13] E. M. Izhikevich, *Dynamical Systems in Neuroscience: The Geometry of Excitability and Bursting* (MIT Press, 2005).
- [14] G. B. Ermentrout and D. H. Terman, *Mathematical Foundations of Neuroscience* (Springer, 2010).
- [15] B. Ermentrout, M. Pascal, and B. Gutkin, *Neural Comp* **13**, 1285 (2001).
- [16] J. Benda and A. V. M. Herz, *Neural Comp.* **15**, 2523 (2003).
- [17] R. Brette and W. Gerstner, *J Neurophysiol* **94**, 3637 (2005).
- [18] W. Gerstner and R. Naud, *Science* **326**, 379 (2009).
- [19] T. Schwalger and B. Lindner, *Eur. Phys. J.-Spec. Top.* **187**, 211 (2010).
- [20] A. Treves, *Network Comput Neural Syst* **4**, 259 (1993).
- [21] W. H. Nesse, L. Maler, and A. Longtin, *Proc Natl Acad Sci USA* **107**, 21973 (2010).
- [22] R. Ratnam and J. B. M. Goense, in *Computational Neuroscience Meeting, Baltimore, MD, USA.* (2004).
- [23] N. Brunel, V. Hakim, and M. J. E. Richardson, *Phys Rev E* **67**, 051916 (2003).
- [24] E. M. Izhikevich, *Neural Networks* **14**, 883 (2001).
- [25] M. P. Nawrot, C. Boucsein, V. Rodriguez-Molina, A. Aertsen, S. Grun, and S. Rotter, *Neurocomp.* **70**, 1717 (2007).
- [26] R. F. Galán, G. B. Ermentrout, and N. N. Urban, *Phys. Rev. Lett.* **94**, 158101 (2005).